

LETTER TO THE EDITOR

Single-cell transcriptomic analysis uncovers intratumoral heterogeneity and drug-tolerant persister in *ALK*-rearranged lung adenocarcinoma

Dear Editor,

Non-small cell lung carcinoma (NSCLC) accounts for more than 85% of all lung cancers [1]. Lung adenocarcinomas (ADCs) arising from never-smokers have been frequently found to be associated with oncogenic driver mutations, including anaplastic lymphoma kinase (*ALK*) rearrangement. Echinoderm microtubule-associated protein-like 4 (*EML4*) is the most common fusion partner of the *ALK* gene [2]. Tyrosine kinase inhibitors (TKIs) are currently the first-line treatment for advanced *EML4-ALK*-rearranged lung ADC. However, NSCLC patients treated with TKIs commonly exhibit disease progression within one to two years of treatment due to the development of acquired resistance [3]. In addition, genotypic diversity among subpopulations of cancer cells contributes to the development of drug insensitivity to other therapeutic options, such as immunotherapy [4], so drug resistance or insensitivity presents the greatest challenge in NSCLC maintenance therapy.

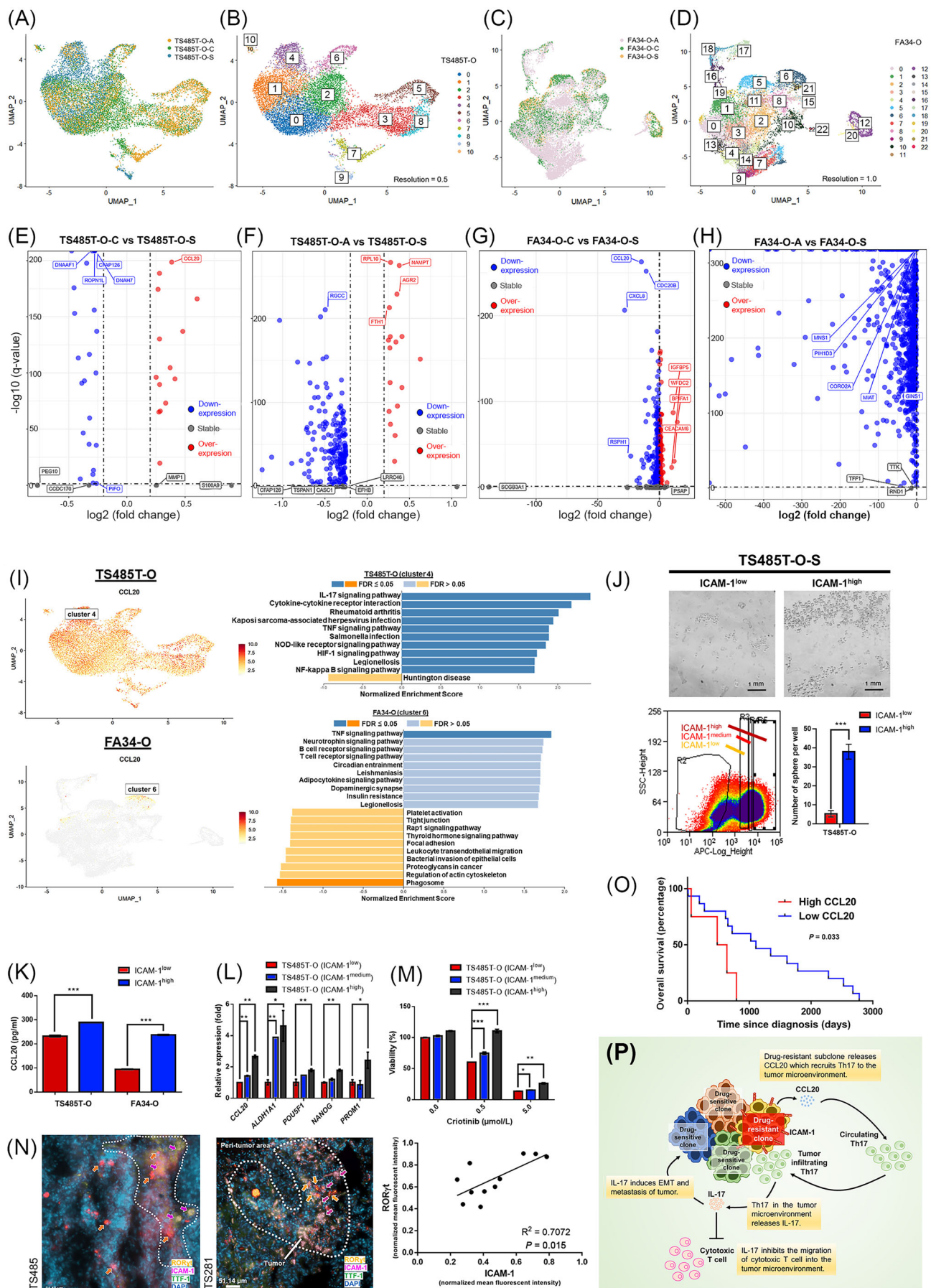
In this study, we hypothesized that drug-tolerant persister (DTP) cells pre-exist among heterogeneous tumor subpopulations and confer drug insensitivity. Two

ALK-rearranged lung cancer organoids (LCOs) (TS485T-organoids (O) derived from a resected primary tumor and FA34-O derived from malignant pleural effusion) were exposed to escalating concentrations of *ALK*-TKIs (Supplementary Figure S1A), leading to the emergence of acquired resistance in four subsequently established drug-resistant LCOs TS485T-O-C, TS485T-O-A, FA34-O-C, and FA34-O-A (-S = drug sensitive; -C = crizotinib resistant; -A = alectinib resistant) (Supplementary Figure S1B). This mimicked the clinical observation of *ALK*-rearranged lung ADC tumors developing acquired resistance after a certain period of *ALK*-TKI treatment. Single-cell RNA-sequencing (scRNA-seq) analysis of two TKI-sensitive and four TKI-resistant tumor organoids of TS485T-O and FA34-O was performed individually. At least 5,000 cells per sample with approximately 12,000 to 31,000 unique molecular index (UMI) counts per cell were sequenced (Supplementary Table S1). Uniform Manifold Approximation and Projection (UMAP) dimensionality reduction analysis allowed the visualization of intratumoral heterogeneity within two groups of samples (Figure 1A-D). Ten clusters from the TS485T-O model (Figure 1A-B) and 21 clusters from the FA34-O model (Figure 1C-D) were partitioned. In both TS485T-O and FA34-O groups, cells from drug-sensitive and drug-resistant LCOs were grouped into separate clusters according to their transcriptomic profiles (Supplementary Figure S2A-B). Differential gene expression (DGE) analysis of drug-resistant and drug-sensitive TS485T-O LCOs revealed that the interleukin-17 (IL-17) signaling pathway was enriched in both crizotinib-resistant and alectinib-resistant tumor organoids (Supplementary Figure S2C-D). Crizotinib-resistant tumor organoids of TS485T-O were characterized by overexpression of the IL-17 pathway component, chemokine (C-C motif) ligand 20 (*CCL20*) (Figure 1E). *CCL20* has been shown to play a role in modulating the tumor immune microenvironment [5]. In alectinib-resistant tumor organoids of TS485T-O, besides the activated IL-17 pathway, upregulation of

Abbreviations: ADCs, Adenocarcinomas; ALDH1A1, Aldehyde dehydrogenase 1 family member A1; *ALK*, Anaplastic lymphoma kinase; CSC, Cancer stem cell; *CCL20*, Chemokine (C-C motif) ligand 20; *CCR6*, chemokine receptor 6; DGE, Differential gene expression; DTP, Drug-tolerant persister; *EGFR*, Epidermal growth factor receptor; *EML4*, Echinoderm microtubule-associated protein-like 4; ELISA, Enzyme-linked immunosorbent assay; *FOS*, Fos Proto-Oncogene; *NANOG*, Homeobox protein *NANOG*; *ICAM-1*, Intercellular adhesion molecule 1; *IL-17*, Interleukin-17; LCOs, Lung cancer organoids; *MUC5AC*, Mucin-5AC; NSCLC, Non-small cell lung carcinoma; *POU5F1*, POU Class 5 Homeobox 1; *PROM1*, Prominin 1; *PTGS2*, Prostaglandin-endoperoxide synthase 2; *ROR γ* , Retinoid-related orphan receptor- γ ; *S100A9*, S100 calcium-binding protein A9; scRNA-seq, Single-cell RNA sequencing; TCGA-LUAD, The Cancer Genome Atlas Lung Adenocarcinoma; Th17, T helper-17 lymphocytes; TKIs, Tyrosine kinase inhibitors; TNF, Tumor necrosis factor; UMI, Unique molecular index; UMAP, Uniform Manifold Approximation and Projection.

This is an open access article under the terms of the [Creative Commons Attribution-NonCommercial-NoDerivs](https://creativecommons.org/licenses/by-nc-nd/4.0/) License, which permits use and distribution in any medium, provided the original work is properly cited, the use is non-commercial and no modifications or adaptations are made.

© 2023 The Authors. *Cancer Communications* published by John Wiley & Sons Australia, Ltd. on behalf of Sun Yat-sen University Cancer Center.



ribosomal protein L10 (*RPL10*), nicotinamide phosphoribosyltransferase (*NAMPT*) and anterior gradient-2 (*AGR2*) were observed (Figure 1F), and the functions of these genes in lung cancer were mentioned in previous studies [6, 7]. In contrast, we found that the actin cytoskeleton regulatory pathway was downregulated in both FA34-O crizotinib-resistant and alectinib-resistant tumor organoids (Supplementary Figure S2E-F). To identify subpopulations of DTP cells and their gene signatures that might have been previously masked in bulk RNA sequencing, the top differentially expressed genes in different clusters were plotted in the single-cell transcriptomic profiles (Supplementary Figure S2G-H). *CCL20* was highly expressed in most TKI-resistant TS485T-O cells, but some clusters with distinctive high expression of *CCL20* (clusters 4 and 10) were found in TKI-sensitive TS485T-O models (Figure 1I, upper panel). In contrast, *CCL20* was weakly expressed in most FA34-O cells, but its expression was higher in cluster 6 (Figure 1I, lower panel). This striking difference in *CCL20* expression between the TS485T-O model (derived from a resected primary tumor) and the FA34-O model (derived from a TKI-naive metastatic tumor) suggest that *CCL20* might play an important role in modulating the tumor immune microenvironment in primary tumors. The IL-17 signaling

pathway and cytokine-cytokine receptor interaction were highly enriched in TS485T-O cluster 4 (Figure 1I, upper right panel), which is mainly enriched in drug-sensitive cells, and a similar enrichment pattern was observed in the DGE analysis of drug-resistant cells (Supplementary Figure S2C-D). In addition, the *CCL20*-expressing cluster (cluster 6) in the FA34-O model (Figure 1I, lower panel) was also characterized by enrichment of the Tumor necrosis factor (TNF) signaling pathway, which was also found in TS485T-O cluster 4 (Figure 1I, upper panel) but not in the DGE analysis of the FA34-O model (Supplementary Figure S2E-F). These data strongly supported the pre-existence of DTP subpopulations.

CCL20, mainly produced by mucosal lymphoid tissues, is a chemokine that directs lymphocyte migration toward epithelial cells. It has been previously reported that *CCL20* expression might contribute to the progression of many cancers [8]. *CCL20* is a secreted protein, so cells cannot be sorted based on the expression of this protein. To characterize the DTP subpopulations, we further explored the DGE profiles of TS485T-O cluster 4 and FA34-O cluster 6 and identified surface markers coexpressed with *CCL20*. We found that intercellular adhesion molecule 1 (*ICAM-1*; CD54), a surface glycoprotein usually

FIGURE 1 Single-cell transcriptomic analysis revealed intratumoral heterogeneity in ALK-TKI-resistant LCOs. UMAP representation of TS485T-O (A-B) or FA34-O (C-D) drug-sensitive or drug-resistant cells colored by the cell of origin (A, C) or by clusters (B, D). Top dysregulated genes and pathways when comparing TS485T-O (E-F) or FA34-O (G-H) models with crizotinib or alectinib-resistant LCOs with sensitive LCOs. *CCL20*-expressing subpopulations and their enriched signaling pathways in TS485T-O (I, upper panel) or FA34-O (I, lower panel) models. (J) A tumor formation assay was performed on ICAM-1 low- or high-expressing cells separated by flow cytometry. The number of spheres was counted after two weeks of cell seeding. (K) *CCL20* levels in conditioned medium were assayed by ELISA 4 days after ICAM-1 sorting. (L) mRNA expression levels of *CCL20* and cancer stem cell markers (*ALDH1A1*, *POU5F1*, *NANOG*, and *PROM1*) in cells with low, medium or high ICAM-1 expression were assayed by real-time RT-PCR after cell sorting. (M) Sensitivity to crizotinib (0.5 or 5 μ mol/L) treatment for 3 days in cells with low, medium, or high ICAM-2 levels were determined by cell viability assay. (N) Colocalization of ICAM-1⁺ (pink) tumor cells and ROR γ t⁺ (orange) Th17 cells in ALK-rearranged primary NSCLC tumor FFPE visualized by multiplexed immunofluorescence staining ($N = 12$). Tumor cells were located by TTF-1 (green) staining, and nuclei were counterstained with DAPI (blue). Representative images of co-localization from two resected tumor tissues, TS485 and TS281, are shown. The number of ROR γ t⁺ lymphocytes and ICAM-1⁺ tumor cells in the tumor area were counted. (O) Association of ALK-rearranged lung ADC patient survival with plasma levels of *CCL20* (ICAM-1^{low}, $n = 15$; ICAM-1^{high}, $n = 4$). * $P < 0.05$; ** $P < 0.01$; *** $P < 0.001$. (P) Hypothetical model showing the role of *CCL20* and its downstream mechanism in modulating the tumor immune microenvironment. Subpopulations of drug-resistant ICAM-1^{high} tumor cells release *CCL20* to recruit Th17 lymphocytes into the tumor microenvironment. Th17 lymphocytes in the tumor bed release IL-17, which can prevent the infiltration of CD8⁺ cytotoxic T cells. IL-17 can also induce EMT and metastasis of tumor cells.

Abbreviations: Anterior gradient 2 (*AGR2*); Chemokine (C-C motif) ligand 20 (*CCL20*); BPI fold containing family A, member 1 (*BPIFA1*); Cancer susceptibility candidate 1 (*CASC1*); Cell division cycle 20B (*CDC20B*); Carcinoembryonic antigen cell adhesion molecule 6 (*CEACAM6*); Cilia and flagella associated protein 126 (*CFAP126*); Coiled-Coil Domain Containing 170 (*CCDC170*); Coronin 2A (*CORO2A*); C-X-C motif chemokine ligand 8 (*CXCL8*); Dynein axonemal assembly factor 1 (*DNAAF1*); Dynein axonemal heavy chain 7 (*DNAH7*); EF-hand domain family member B (EFHB); Ferritin heavy chain 1 (*FTH1*); GINS complex subunit (*GINS1*); Hypoxia-inducible factors (*HIF*); Leucine Rich Repeat Containing 46 (*LRRC46*); Matrix metalloproteinase 1 (*MMP1*); Meiosis specific nuclear structural 1 (*MNS1*); Nicotinamide phosphoribosyltransferase (*NAMPT*); Nucleotide oligomerization domain (*NOD*); Myocardial infarction associated transcript (*MIAT*); Paternally Expressed 10 (*PEG10*); PIH1 domain containing 3 (*PIH1D3*); Primary cilia formation (*PIFO*); Prosaposin (*PSAP*); Ras-proximate-1 (*RAP1*); Radial spoke head component 1 (*RSPH1*); Regulator of cell cycle (*RGCC*); Rho family GTPase 1 (*RND1*); RhoGTPase associated tail protein 1 like (*ROPN1L*); Ribosomal Protein L10 (*RPL10*); Insulin like growth factor binding protein 5 (*IGFBP5*); Intercellular adhesion molecule 1 (*ICAM-1*); Interleukin-17 (*IL-17*); S100 Calcium Binding Protein A9 (*S100A9*); Trefoil factor 1 (*TFF1*); Tetraspanin 1 (*TSPAN1*); Threonine tyrosine kinase (TTK); T helper-17 lymphocytes (Th17); WAP four-disulfide core domain protein 2 (*WFDC2*)

expressed on endothelial cells but previously identified as a cancer stem cell (CSC) marker [9, 10], was also highly expressed in *CCL20*-expressing clusters (Supplementary Figure S3). To investigate the tumorigenicity of tumor subpopulations expressing different levels of *ICAM-1*, tumor sphere formation assays and qRT-PCR were performed on *ICAM-1*^{high}, *ICAM-1*^{medium} and *ICAM-1*^{low} cells separated by flow cytometry. TS485T-O cells with high *ICAM-1* demonstrated a much stronger sphere formation ability (Figure 1J). Cells with high *ICAM-1* expression released more *CCL20* than *ICAM-1*^{low} cells (Figure 1K). We also found that *ICAM-1*^{high} cells expressed higher levels of CSC marker genes, including aldehyde dehydrogenase 1 family member A1 (*ALDH1A1*), POU Class 5 Homeobox 1 (*POU5F1*), Homeobox protein NANOG (*NANOG*) and Prominin 1 (*PROM1*) (Figure 1L), and were characterized by a stronger resistance to crizotinib (Figure 1M). All these data indicate the strong tumorigenicity of *ICAM-1*^{high} and *CCL20*-releasing tumor cell subpopulations in *ALK*-rearranged lung ADCs.

Analysis in the Cancer Genome Atlas Lung Adenocarcinoma (TCGA-LUAD) cohort showed that higher tumor *CCL20* expression levels were associated with poor survival (Supplementary Figure S4). A statistically significant difference in *CCL20* expression levels was found when comparing normal lung tissues with tumor tissues from non-smokers. These results suggested that tumor *CCL20* expression may be a prognostic biomarker in non-smokers with NSCLC. To evaluate the role and clinical relevance of the *CCL20*-expressing subpopulation in primary tumors that could be DTP cells, multiplexed immunofluorescence staining was used to evaluate the spatial co-localization of *ICAM-1*⁺ tumor cells and retinoid-related orphan receptor- γ ⁺ T helper 17 (ROR γ ^t Th17) lymphocytes in resected primary tumor tissues (Figure 1N). *CCL20* is a chemokine that directs chemokine receptor 6 (*CCR6*)-expressing lymphocytes, including Th17 lymphocytes, to migrate toward epithelial cells. The frequency of *ICAM-1*⁺ tumor cells correlated positively with the number of ROR γ ^t Th17 lymphocytes, suggesting that Th17 lymphocytes are actively recruited into the tumor microenvironment by *ICAM-1*⁺ tumor subpopulations. In addition, plasma levels of *CCL20* from 21 patients with advanced *ALK*-rearranged NSCLC were assayed with enzyme-linked immunosorbent assay (ELISA). Similar to tumor *CCL20* expression in TCGA-LUAD, high plasma *CCL20* was associated with poor survival (Figure 1O). These data suggested that although *CCL20* might not be responsible for mediating TKI resistance, infiltration of Th17 lymphocytes may be key to the development of drug insensitivity to immune checkpoint inhibitor therapy (Figure 1P).

In conclusion, our scRNA-seq data identified a subpopulation of *ALK*-TKI-resistant DTP lung ADC cells that

might contribute to the development of TKI resistance and modulation of the tumor immune microenvironment.

DECLARATIONS

AUTHOR CONTRIBUTIONS

Hoi-Hin Kwok: laboratory experiment coordination and supervision and manuscript writing. Huiyu Li and Luc Girard: single-cell RNA computational analysis. Jiashuang Yang, Junyang Deng, and Nerissa Chui-Mei Lee: laboratory experiments. Timmy Wing-Kuk Au, Alva Ko-Yung Sit and Michael Kuan-Yew Hsin: surgical management of recruited subjects. Lydia Wai-Ting Cheung and Stephanie Kwai-Yee Ma: assistance in the establishment of LCOs. Junya Fujimoto and Ignacio Ivan Wistuba: cytological and histological evaluation. Boning Gao and John Dorrance Minna: data analysis and manuscript drafting. David Chi-Leung Lam: overall conceptualization, manuscript drafting and revision, and analysis of results.

ACKNOWLEDGMENTS

Not applicable.

CONFLICTS OF INTEREST STATEMENT

JDM receives licensing royalties from the United States National Institute of Health and the University of Texas Southwestern Medical Center at Dallas for the distribution of human tumor cells and human bronchial epithelial cell strains. The other authors declare that they have no competing interests.

FUNDING

The research work described in this report was supported by the Lee and the Ho Families Respiratory Research Fund (research donation to DCL). National Natural Science Foundation of China (Grant# 82022078 to LWTC). United States National Cancer Institute Lung Cancer Specialized Program in Research Excellence (SPORE) P50 (CA070907 to JDM).

ETHICAL APPROVAL AND CONSENT TO PARTICIPATE

The study protocol was approved by the Ethics Committee of the University of Hong Kong and the Hong Kong Hospital Authority of Hong Kong West Cluster Institutional Review Board (IRB Reference Number UW 16-104). Informed consent was obtained from all the participants.

CONSENT FOR PUBLICATION

Not applicable.

DATA AVAILABILITY STATEMENT

All the data supporting the conclusions of this article are included within the article. Data for single-cell sequencing

were deposited in National Center for Biotechnology Information Gene Expression Omnibus NCBI-GEO repository (GSE223779).

Hoi-Hin Kwok¹ 
 Huiyu Li²
 Jiashuang Yang¹
 Junyang Deng¹
 Nerissa Chui-Mei Lee¹
 Timmy Wing-Kuk Au³
 Alva Ko-Yung Sit³
 Michael Kuan-Yew Hsin³
 Stephanie Kwai-Yee Ma⁴
 Lydia Wai-Ting Cheung⁴
 Luc Girard²
 Junya Fujimoto⁵
 Ignacio Ivan Wistuba⁵
 Boning Gao²
 John Dorrance Minna²
 David Chi-Leung Lam¹ 

¹*Department of Medicine, Li Ka Shing Faculty of Medicine, University of Hong Kong, Hong Kong SAR, P. R. China*

²*Nancy B. and Jake L. Hamon Center for Therapeutic Oncology Research, University of Texas Southwestern Medical Center, Dallas, Texas, USA*

³*Cardiothoracic Surgical Department, Queen Mary Hospital, Hong Kong SAR, P. R. China*

⁴*School of Biomedical Sciences, Li Ka Shing Faculty of Medicine, The University of Hong Kong, Hong Kong SAR, P. R. China*

⁵*Department of Translational Molecular Pathology, Division of Pathology/Lab Medicine, University of Texas MD Anderson Cancer Center, Houston, Texas, USA*

Correspondence

David Chi-Leung Lam, Department of Medicine, Li Ka Shing Faculty of Medicine, University of Hong Kong, Hong Kong SAR 999077, P. R. China
 Email: dcllam@hku.hk

ORCID

Hoi-Hin Kwok  <https://orcid.org/0000-0002-6902-8402>

David Chi-Leung Lam  <https://orcid.org/0000-0002-0004-2660>

REFERENCES

1. Tsao MS, Nicholson AG, Maleszewski JJ, Marx A, Travis WD. Introduction to 2021 WHO Classification of Thoracic Tumors. *J Thorac Oncol.* 2022;17(1):e1-e4.
2. Soda M, Choi YL, Enomoto M, Takada S, Yamashita Y, Ishikawa S, et al. Identification of the transforming EML4-ALK fusion gene in non-small-cell lung cancer. *Nature.* 2007;448(7153):561-6.
3. Katayama R, Friboulet L, Koike S, Lockerman EL, Khan TM, Gainor JF, et al. Two novel ALK mutations mediate acquired resistance to the next-generation ALK inhibitor alectinib. *Clin Cancer Res.* 2014;20(22):5686-96.
4. Oya Y, Kuroda H, Nakada T, Takahashi Y, Sakakura N, Hida T. Efficacy of Immune Checkpoint Inhibitor Monotherapy for Advanced Non-Small-Cell Lung Cancer with ALK Rearrangement. *Int J Mol Sci.* 2020;21(7):2623.
5. Fan T, Li S, Xiao C, Tian H, Zheng Y, Liu Y, et al. CCL20 promotes lung adenocarcinoma progression by driving epithelial-mesenchymal transition. *Int J Biol Sci.* 2022;18(11):4275-88.
6. Okumura S, Sasaki T, Minami Y, Ohsaki Y. Nicotinamide phosphoribosyltransferase: a potent therapeutic target in non-small cell lung cancer with epidermal growth factor receptor-gene mutation. *J Thorac Oncol.* 2012;7(1):49-56.
7. He J, Fu Y, Hu J, Chen J, Lou G. Hypomethylation-Mediated AGR2 Overexpression Facilitates Cell Proliferation, Migration, and Invasion of Lung Adenocarcinoma. *Cancer Manag Res.* 2021;13:5177-85.
8. Peng DH, Rodriguez BL, Diao L, Gaudreau P-O, Padhye A, Konen JM, et al. Th17 cells contribute to combination MEK inhibitor and anti-PD-L1 therapy resistance in KRAS/p53 mutant lung cancers. *Nat Commun.* 2021;12(1):2606.
9. Song M, Ping Y, Zhang K, Yang L, Li F, Zhang C, et al. Low-Dose IFN γ Induces Tumor Cell Stemness in Tumor Microenvironment of Non-Small Cell Lung Cancer. *Cancer Res.* 2019;79(14):3737-48.
10. Taftaf R, Liu X, Singh S, Jia Y, Dashzeveg NK, Hoffmann AD, et al. ICAM1 initiates CTC cluster formation and trans-endothelial migration in lung metastasis of breast cancer. *Nat Commun.* 2021;12(1):4867.

SUPPORTING INFORMATION

Additional supporting information can be found online in the Supporting Information section at the end of this article.